J. Chem. Sci. (2020)132:56
https://doi.org/10.1007/s12039-020-1756-9
© Indian Academy of Sciences

REGULAR ARTICLE

Synthesis and application of carboxyethylthiosuccinic acid by thiol-ene click reaction: as a novel rust remover with corrosion inhibition properties

HUAJING GAO[a], NING XIE[a], JIANXIN ZHANG[a], JIAN SUN[a,*], JIANLIN ZHANG[b] and ZHAOHUI JIN[a]

[a]Jilin Institute of Chemical Technology, Institute of Petrochemical Technology, Jilin 132022, China
[b]Yellow River Delta Jingbo Chemical Research Institute Co. Ltd., Shandong 256500, China
E-mail: sunjian6225@126.com

MS received 2 September 2019; revised 4 November 2019; accepted 24 November 2019

Abstract. Carboxyethylthiosuccinic acid (CETSA) was synthesized by thiol-ene click reaction and determined by various characterization methods, such as ^{1}H NMR, IR and TG. A novel rust remover with corrosion inhibition was prepared by using CETSA as the main component. The results of rust removal were tested by the difference method and intuitive comparison method, and its rust removal mechanism was explored. The corrosion inhibition effect of the composite reagent for A3 steel in 1 M HCl solution was investigated by static weight loss test, the adsorption isotherm was calculated and fitted.

Keywords. CETSA; rust remover; steel; corrosion inhibition.

1. Introduction

Metals are one of the most common materials in the modern industry due to its malleability, conductivity and cost-effectiveness. However, the long-term use of metal materials will face the problem of rust, especially, metal equipment rust will bring economic losses and safety risks in industrial production.[1] Pickling technology is the process of removing rust on the metal surface by using an acid solution. At present, a strong acid is widely used in traditional rust remover process, and the effect of rust removal is achieved by reacting with metal oxide.[2–5] However, in this process, it will cause corrosion to the metal, and it is easy to form acid fog, which is harmful to the environment, the human body and surrounding equipment. The use of corrosion inhibitor is the most simple and effective way to solve the problem of metal corrosion.[6,7] The mechanism of corrosion inhibitor is to form a protective film by adsorbing the active site on the metal surface to inhibit hydrogen ion contact with the metal surface. The type of corrosion inhibitor can be divided into inorganic corrosion inhibitor,[8] organic corrosion inhibitor[9–16] and mixed substance corrosion inhibitor, in which the organic corrosion inhibitor is mainly heterocyclic compounds. The heteroatoms of organic corrosion inhibitors have lone pair electrons, which can form coordination bonds with the empty orbitals of transition metals, thus forming a barrier on the metal surface.[17–28] In the early stage, phosphorus-containing compounds and toxic inorganic salts were mainly used as corrosion inhibitors,[29] which polluted the environment. In recent years, some plant extracts have been reported as corrosion inhibitors, which are green and environmentally friendly, but expensive and difficult to industrialize.[30–35] Therefore, at present, a new type of rust remover is needed, which can have an excellent performance of rust removal in the pickling process without excessive corrosion of metals.

Click reaction is a simple reaction with mild reaction conditions and high yield. It is commonly used in polymer modification, biomedicine, basic chemical synthesis and other fields.[36–40] In this paper, CETSA was synthesized by thiol-ene click reaction. The structure of the product was determined by ^{1}H NMR and IR. The thermal decomposition temperature of

*For correspondence

Electronic supplementary material: The online version of this article (https://doi.org/10.1007/s12039-020-1756-9) contains supplementary material, which is available to authorized users.

Published online: 16 March 2020

CETSA was analyzed by TG. Due to the strong acidity and special coordination molecular structure of CETSA, it may have the ability of chelating metal ions and corrosion inhibition. Therefore, a new type of rust remover with corrosion inhibition was prepared by using CETSA as the main component. The rust removal performance was tested compared with 10% HCl solution and commercial rust remover. The rust removal rate was calculated by the difference method, and the rust removal degree was observed by intuitive comparison method. The rust before, and after rust removal was characterized by XRD. The corrosion current density of the steel sheet in the rust remover was analyzed by polarization curve test, and the surface morphology of steel sheet after rust removal was observed by SEM. At the same time, the corrosion inhibition performance of the reagent on A3 steel in 1M HCl solution was studied by static weight loss method. In order to further understand the adsorption behavior of molecules on the steel sheet, the adsorption model was fitted and analyzed.

2. Experimental

2.1 *Materials and physical measurements*

The test material for this study was commercially available as A3 steel. Maleic acid, β-mercaptopropionic acid, trimethylamine (NEt_3), triethanolamine, sodium hydroxide, sodium carbonate, sodium chloride, methenamine and sodium lauryl sulfate were purchased from Energy Chemical, 30% hydrogen peroxide solution was purchased from Tianjin Yongda Chemical Reagent Co. Ltd., SepliteLSZ-106S anion exchange resin was purchased from Xi'an Sunresin New Materials Co. Ltd., hydrochloric acid was purchased from Beijing Chemical Works. Commercial rust remover was purchased from Guangzhou End Chemical Technology Co. Ltd. For the tests, the sample surfaces were polished by sandpaper, washed by distilled water, petroleum ether and ethanol in turn, and then dried in the oven. IR was carried out in the range of 500–4000 cm^{-1} by Fourier transform infrared spectroscopy with KBr tablet pressing method. Deuterium substituted water was used as a solvent to obtain ^1H NMR spectra by 400 MHz NMR spectrometer. Thermogravimetric analysis (TG) was measured in a Q35 instrument. The product was loaded in a platinum crucible and heated in N_2 (50 $mL{\cdot}min^{-1}$) at a heating rate of 10 $°C{\cdot}min^{-1}$ from 20 to 300 °C.

2.2 *Synthesis of CETSA*

CETSA was synthesized according to the following step and used as the main component for rust remover (Scheme 1). Maleic acid was dissolved in 50 mL water and mixed with 0.2 mol β-mercaptopropionic acid, then 5 mol% catalyst was added. The reaction mixture was stirred and heated to 80–95 °C for 2.5–3.5 h. The mixed reaction solution was cooled to crystallize at 8 °C. The crude product of CETSA as the crystal was obtained by decompression and filtration. After recrystallization, the product was dried to remove moisture. The effects of reaction temperature, the molar ratio of raw materials, reaction time and the selection of catalyst on the yields were investigated. ^1H NMR (400 Hz, $CDCl_3$) δ 3.68 (dd, 1H, J = 5.6, 9.4 Hz), 2.87 (m, 3H), 2.73 (m, 1H), 2.63 (m, 2H). IR (KBr, cm^{-1}): 2671(O-H), 1693(C=O), 1419(O=C-O), 1311(H-C-H), 670(C-S-C), 618(CH-S). The spectral data were in agreement with the structure of this compound.

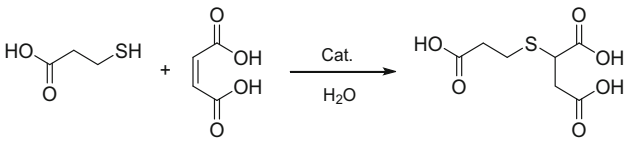

Scheme 1. The synthesis of CETSA.

2.3 *Determination of rust removal rate*

The rust remover was prepared by adding the mixture of 10% CETSA, 0.5% methenamine and 0.2% sodium lauryl sulfate to the aqueous solution. Difference method was carried out using A3 steel specimens with a surface area of 0.005 m^2 to determine the rust removal rate. Steel sheets were rusted quickly by steeping in a mixed solution of 30% hydrogen peroxide solution and sodium chloride, then soaked in 10% HCl solution, commercial rust remover and the rust remover which contained CETSA until the rust on the surface completely disappeared. The specimens were cleaned in distilled water and dried in drying box, the weight before and after the test were recorded. The rust removal rates V which derived from the weight loss method were calculated using equations (1).

$$V = \frac{m_0 - m_1}{ts} \tag{1}$$

Where, s is the sample area immersed in rust remover (m^2), t represents the immersion time (h) and m_0 is the weight of the sample before the test (g), m_1 is the weight of the sample after the test (g).

The solution after rust removal was filtered and characterized by XRD of the residue. CHI760e electrochemistry workstation was used to determine the electrochemical behavior of a traditional three-electrode cell (the rusty A3 steel with exposed area of 1 cm^2 was used as the working electrode, platinum electrode was used as an auxiliary electrode, and standard calomel electrode (SCE) was used as reference electrode) in three kinds of rust remover. Tafel curves were obtained by changing the electrode potential automatically from 0 to 800 mV versus corrosion potential

(E_{corr}) at a scan rate of 1 mV·s^{-1}. Surface topography of A3 steel and that treated with three kinds of rust remover were observed by using SEM.

2.4 *Determination of corrosion inhibition efficiency*

The corrosion inhibition performance of the rust remover which contained CETSA was determined by static weight loss method: the A3 steel was polished with sandpaper, the polished test piece was washed with deionized water, petroleum ether and ethanol in turn, and then dried with drying box, for drying 5 min, and the size of the test piece was measured.

1 M HCl aqueous solution was prepared and the rust remover which contained CETSA as corrosion inhibitor was added. The steel sheets were fastened with cotton thread and soaked in the solution, and they were left alone for 20 h. Then, the surface of the test piece washed with distilled water, petroleum ether and ethanol in turn, the steel sheets were dried and weighed on the electronic balance, the relevant data were recorded.

The obtained data were listed in Table 3 and the corrosion rate and corrosion inhibition efficiency were calculated by equation (2) and (3), respectively:

$$C_r = \frac{W_0 - W_1}{TA} \tag{2}$$

Where, W_0 is the weight of the sample before corrosion (g), W_1 is the weight of the corroded sample (g), T is the time of immersion (h), and A is the area of the specimen exposed to the corrosive solution (m^2).

$$\eta = \frac{C_r - C_r'}{C_r} \tag{3}$$

Where η is the corrosion inhibition efficiency, C_r and C_r' represent the corrosion rate in the absence and presence of inhibitor.

3. Results and Discussion

3.1 *Condition optimization and synthesis mechanism of CETSA*

The effect of reaction conditions on the yield of CETSA is investigated and the results are shown in Table 1. Among the different catalysts, the best yield of product is obtained by using NEt_3. Notably, increasing the amount of maleic acid give an even better yield. The highest product yield (87%) can be obtained by 1.1 equivalent maleic acid reacts with 1 equivalent β-mercaptopropionic acid at 90 °C for 3 h. On the basis of these results and previous work, we propose the following catalytic mechanism (Scheme 2). β-mercaptopropionic acid first reacts with NEt_3 to form the corresponding triethylammonium cation **A** and thiolate anion **B**. As a powerful nucleophile, the thiolate anion adds into the activated C=C bond-forming a carbon-centred anion intermediate **C** which is a very strong base.[41] This anion picks up a proton from a thiol or from the ammonium cation **A** to generate the thiol-ene product. Therefore, the carbanion as a stronger base is formed by using a relatively weak base (NEt_3) in this catalytic cycle.

3.2 *Thermal stability analysis of CETSA*

In order to research the thermal stability and the thermal decomposition temperature of CETSA, the product is characterized by TG and the result is shown in Figure 1. According to the result of TG, there is a strong peak of weight loss between 160–170 °C, which is attributed to CETSA decomposition, and CETSA is completely decomposed at 210 °C. Under other

Table 1. Optimization of reaction conditions for synthesis of CETSA.[a]

Entry	Catalyst	T (°C)	Time (h)	Yield (%)
1	TEOA	90	3	61
2	NaOH	90	3	80
3	Na_2CO_3	90	3	59
4[b]	SepliteLSZ-106S anion exchange resin	90	3	81
5	NEt_3	90	3	83
6[c]	NEt_3	90	3	68
7[d]	NEt_3	90	3	87
8[d]	NEt_3	80	3	76
9[d]	NEt_3	85	3	82
10[d]	NEt_3	95	3	86
11[d]	NEt_3	90	2.5	77
12[d]	NEt_3	90	3.5	74

[a]Reaction conditions: Maleic acid (0.21 mol), β-mercaptopropionic acid (0.2 mol), H_2O (50 mL), catalyst (5 mol%); [b]Seplite LSZ-106S anion exchange resin (0.5 g); [c]Maleic acid (0.2 mol); [d]Maleic acid (0.22 mol); TEOA = triethanolamine.

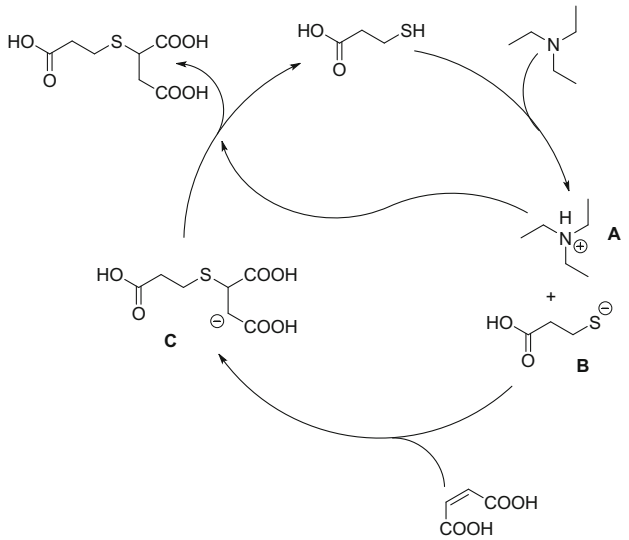

Scheme 2. Proposed reaction mechanism of β-mercaptopropionic acid with maleic acid.

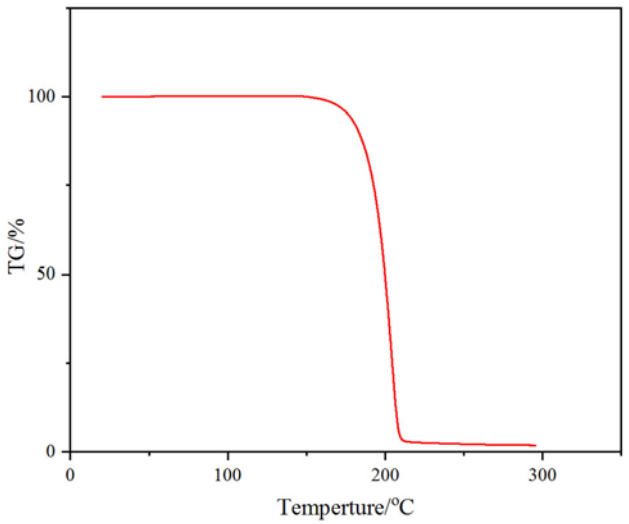

Figure 1. TG spectra of CETSA.

temperature conditions, there is no weight loss peak, especially at 100 °C, which indicates that the product CETSA does not contain bound water.

3.3 *Rust removal performance analysis*

The rust removal rate of the three rust removal agents at different temperature is shown in Table 2. With the increase of temperature, the rust removal rate of 10% HCl solution and commercial rust remover were increased significantly, which may be because the increase of temperature accelerated the decomposition reaction of strong acid and metal oxide. The surface of A3 steel is treated with three rust removers is shown in Figure 2. The surface of A3 steel treated with 10% HCl solution and commercial rust remover are severely corroded and blackens, while the rust remover which contained CETSA can keep the metal shiny after rust removal. The results indicate that rust removal rate of the rust remover which contained CETSA is less affected by temperature and will not seriously corrode the metal compared with the other two kinds of rust remover.

The XRD images of the rust on A3 steel sheet and conversion product after rust removal are shown in Figure 3. The absorption peak of conversion product obtained after rust removal is obviously different from that of rust. The state of the three kinds of rust removers after rust removal is shown in Figure 4. The color of 10% HCl solution (Figure 4a) and commercial rust remover (Figure 4b) is yellow after rust removal due to it contains Fe^{3+}. In contrast, rust removers which contained CETSA peel oxides off metal surfaces to form sediment (Figure 4c), thus, the solution does not appear yellow and transparent after rust removal. Although the rust removal mechanism of CETSA is not clear at present, it is certain that the rust

Table 2. Rust removal rate of three kinds of rust remover at different temperatures.

Solution	T/°C	m_0/g	m_1/g	t/h	V/g·h^{-1}·m^{-2}
The rust remover which contained CETSA	25	20.5612	20.4268	0.1667	161.28
	35	20.6744	20.4428	0.1667	277.92
	45	20.3200	20.0632	0.1667	308.16
	55	20.4708	20.1948	0.1667	331.20
10% HCl solution	25	20.6884	20.4668	0.2000	221.60
	35	20.3424	20.0244	0.2000	318.00
	45	20.3288	19.6004	0.2000	728.40
	55	20.5648	20.0004	0.1000	1128.80
Commercial rust remover	25	20.7788	20.6024	0.2000	176.40
	35	20.8240	20.5168	0.2000	307.20
	45	20.3008	19.6176	0.2000	683.20
	55	20.1664	19.6208	0.1000	1091.20

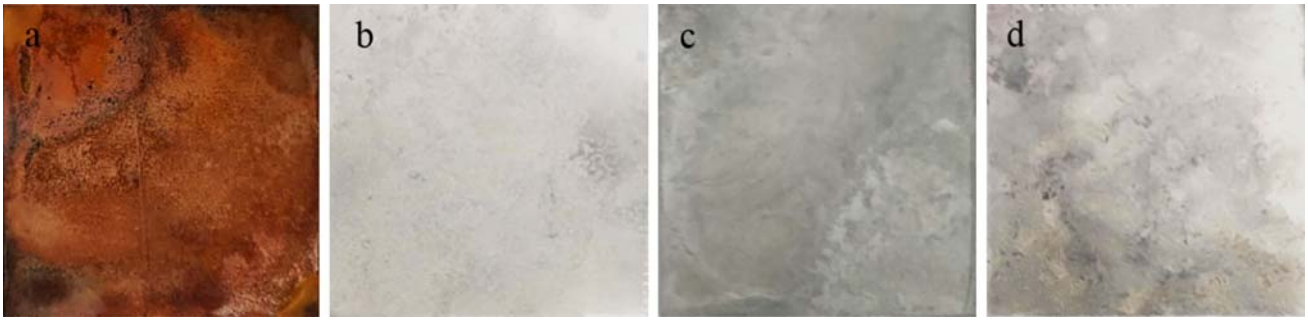

Figure 2. (a) Picture of rusty A3 steel sheet, (b) that treated with the rust remover which contained CETSA, (c) with 10% HCl solution, (d) and with commercial rust remover.

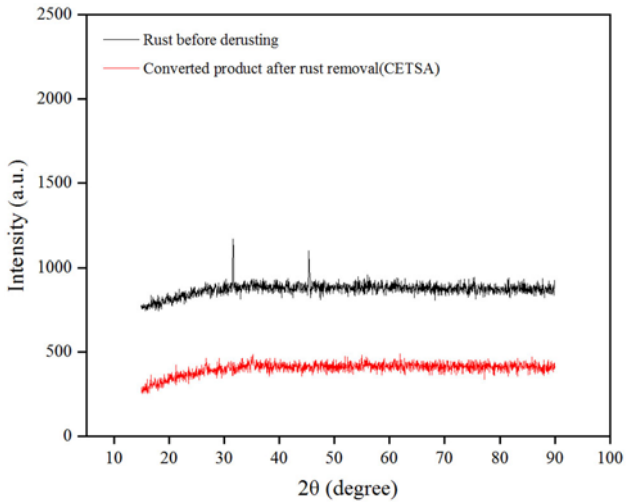

Figure 3. XRD images of the rust on A3 steel sheet and conversion product after rust removal.

has changed after treatment (Figure 4c). The existence of weight difference between the rust scale before removal (0.1396 g) and the filtered sediment (0.0718 g) was proved by weighing, this indicated that part of the rust scale may be dissolved in the rust remover which contained CETSA. Therefore, this process is not simply mechanical rust removal. Rust scale is a loose and porous mixture which contained α-FeOOH, γ-FeOOH and Fe_3O_4.[4] CETSA may penetrate into the rust scale and reacts with it to make it fall off the metal surface.

The polarization curves of rusty A3 steel in three rust removers are shown in Figure 5. The corrosion potential (E_{corr}), corrosion current density (i_{corr}), the slope of cathode Tafel (β_c) and slope of anode Tafel (β_a) of the system can be obtained by analyzing the polarization curve with origin software, and the data

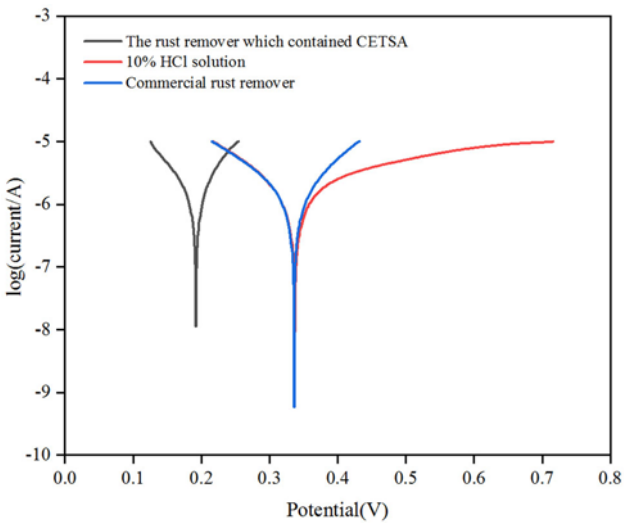

Figure 5. Tafel polarization curves of rusty A3 steel in rust remover solution.

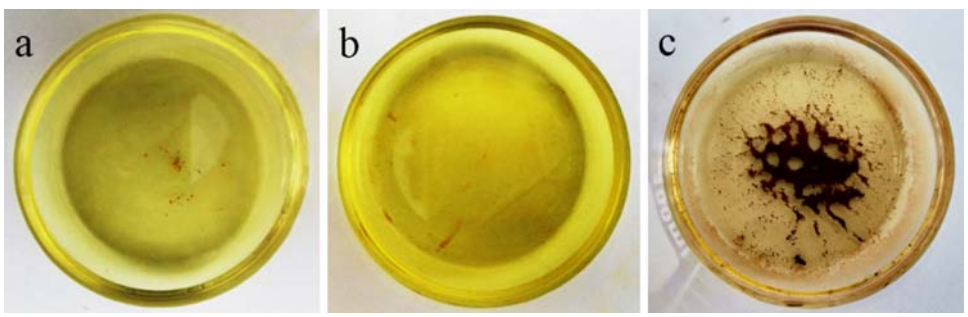

Figure 4. Picture of 10% HCl solution (a), commercial rust remover (b), the rust remover which contained CETSA (c) after rust removal.

Table 3. Fitted tafel polarization curve parameters for rusty A3 steel in rust remover solutions.

Solution	E_{corr} (mV)	β_a (V/dec)	$-\beta_c$ (V/dec)	i_{corr} (μA cm^{-2})
The rust remover which contained CETSA	192	20.3	18.0	0.78
10% HCl solution	336	2.1	7.6	2.01
Commercial rust remover	337	9.1	7.1	1.40

are shown in Table 3. The corrosion current density of 10% HCl solution and commercial rust remover are much higher than that of the rust remover which contained CETSA. The corrosion current density of the rust remover which contained CETSA is very small, which can still achieve the rust removal effect. This result proves that the rust removal mechanism of the rust remover which contained CETSA is different from that of traditional strong acid rust remover, which relies on acid dissolving rust.

3.4 *Surface analysis*

The SEM images of the surface of A3 steel treated with three rust removers are shown in Figure 6. The protective layer formed during the rust removal process is confirmed by SEM images. Aggressive attack of commercial rust remover and 10% HCl solution on the A3 steel surface after removing rust are shown in Figure 6(c) and (d), the distribution of corrosion products is extremely uneven, and the metal surface is seriously damaged. The result indicates that 10% HCl solution and commercial rust remover corrode the metal while achieving the effect of rust removal. Figure 6(b) shows that a thin film is formed on the surface to protect the metal after the rust removal process with the rust remover which contained CETSA. According to the results of SEM, the rust remover which contained CETSA is different from the other two rust removers, which can protect effectively the metal from corrosion in the process of rust removal.

3.5 *Corrosion inhibition performance analysis*

The effects of adding different concentrations of corrosion inhibitors at different temperatures on inhibition efficiency are shown in Figure 7. It is worth noting that corrosion inhibition can be effectively achieved by adding a small amount of the rust remover

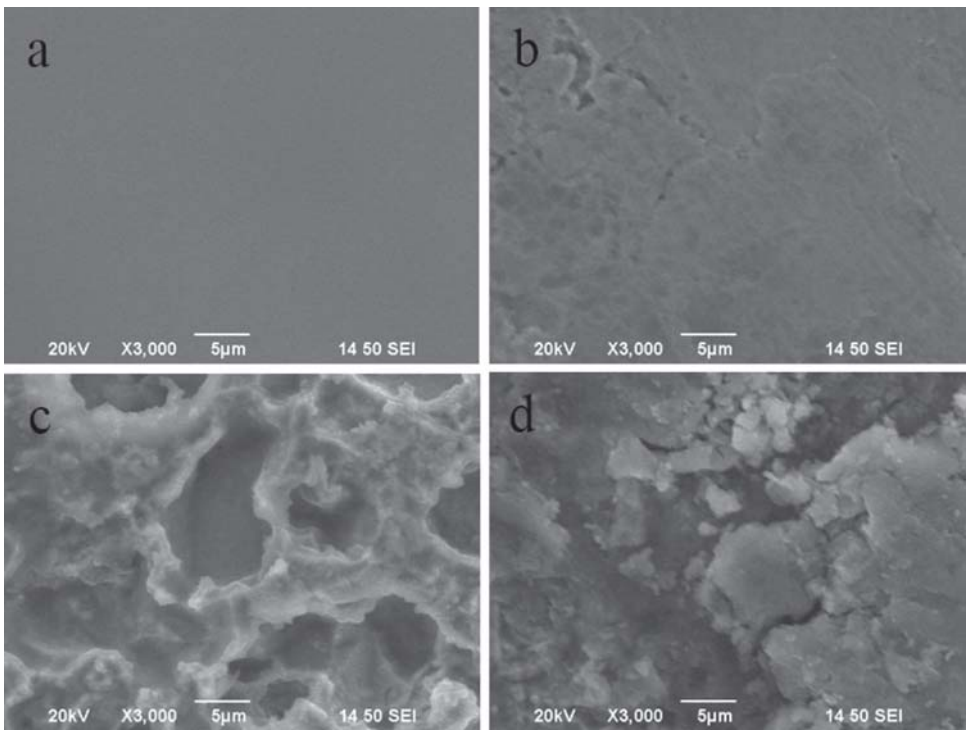

Figure 6. SEM images of blank (a) and steel treated with the rust remover which contained CETSA (b), with 10% HCl solution (c), with commercial rust remover (d).

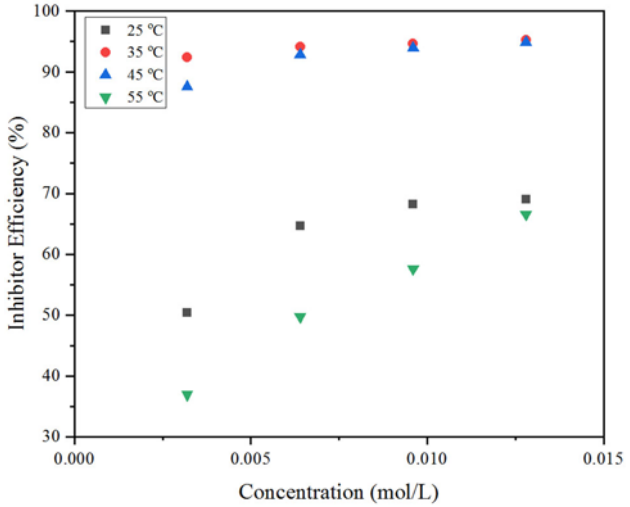

Figure 7. Effect of concentration of the rust remover which contained CETSA on inhibition efficiency at various temperatures.

which contained CETSA, and even the inhibition efficiency can reach more than 90% at 35 °C. Both CETSA and methenamine play an important role in the whole corrosion inhibitor system, the two compounds have polar groups centered on S and N atoms with high electronegativity, respectively. These central atoms can form coordination bonds with the unoccupied empty d orbitals of transition metal atoms and form an adsorption film at the metal interface to inhibit corrosion of metal. The corrosion inhibition efficiency significantly decreases at 55 °C, which may be due to the reaction of methenamine with a part of CETSA to form quaternary ammonium salt and lose the corrosion inhibition effect when the temperature rises to a certain extent.

3.6 *Adsorption isotherm analysis*

In order to explore the adsorption behavior of inhibitor molecules on the surface of A3 steel sheet, the data of concentration of inhibitor (c) and surface coverage (θ) were substituted into several common models, such as Langmuir, Frumkin and Freundlich, and the adsorption isotherm was fitted and analyzed. The model expressions could be found in formulas (4), (5) and (6).

$$\frac{c}{\theta} = \frac{1}{K} + c \tag{4}$$

$$\ln\left[\frac{\theta}{c(1-\theta)}\right] = lnK + 2a\theta \tag{5}$$

$$ln\theta = lnK + nlnc \tag{6}$$

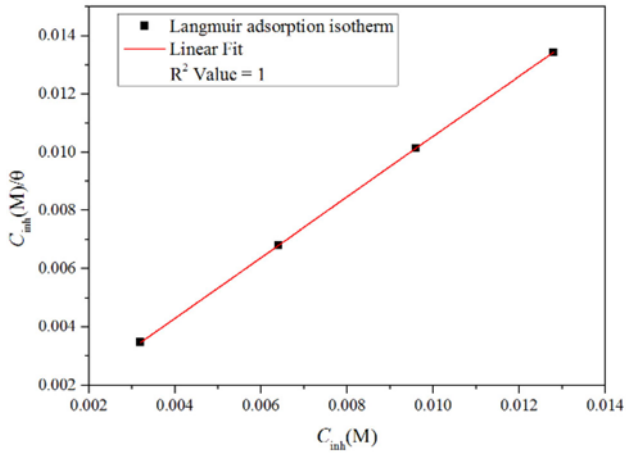

Figure 8. The Langmuir adsorption isotherm of the rust remover which contained CETSA on the surface of A3 steel in 1 M HCl solution at 35 °C.

The linear correlation between c/θ and c is found to be the best through calculation. It can be seen that the adsorption behavior of the inhibitor on the surface of A3 steel is the most consistent with the Langmuir isotherm. The linear correlation coefficients (R^2) of c/θ and c are 0.999, 1, 1 and 0.998 at 25 °C–45 °C, which was obtained by Excel software fitting. The Langmuir adsorption isotherm of the rust remover which contained CETSA on the surface of A3 steel at 35 °C in 1 M HCl solution is shown in Figure 8.

4. Conclusions

In summary, CETSA was successfully synthesized by using the thiol-ene click reaction and was investigated as the main component of rust remover. Findings could be concluded as follows:

(1) The highest yield of CETSA was obtained by using NEt_3 as a catalyst, and the structure of the product was proved to be correct by ^1H NMR and IR. The result of TG showed that the product did not contain bound water and was decomposed between 160–170 °C.
(2) The rust remover was prepared by adding the mixture of 10% CETSA, 0.5% methenamine and 0.2% sodium lauryl sulfate to an aqueous solution. The rust removal rate of the rust remover which contained CETSA was less affected by temperature and would not seriously corrode the metal compared with 10% HCl solution and commercial rust remover.
(3) Some of the rust scale was dissolved by the rust remover which contained CETSA, and the rest formed precipitation. The results of XRD indicated

that the precipitates formed by falling off from the metal surface have changed, and the structure was different from the rust before rust removal. The polarization curve parameters were shown that the corrosion current density of the rust remover which contained CETSA was lower than that of 10% HCl solution and commercial rust remover when the rust removal effect was achieved, which indicated that the former is less corrosive to metals in the rust removal process.

(4) The surface morphology of A3 steel after rust removal was observed by SEM. It was found that the rust remover which contained CETSA could form an adsorption film on the metal surface in the process of rust removal to protect the metal from corrosion.

(5) The rust remover which contained CETSA as a novel corrosion inhibitor for A3 steel in 1 M HCl solution was investigated by static weight loss test. Corrosion inhibition can be effectively achieved by adding a small amount of the rust remover which contained CETSA, and even the inhibition efficiency can reach more than 90% at 35–45 °C. The adsorption behavior was determined to be the most consistent with the Langmuir adsorption isotherm through calculation and fitting.

Supplementary Information (SI)

All additional information pertaining to experimental data and characterization of using ^{1}H NMR and IR spectra are given in Figures S1–S2. The data of corrosion rate and surface coverage are shown in Table S1. The calculation results of the adsorption isotherm are shown in Table S2. The components of the commercial rust remover are shown in Table S3. The effect of percentages of sodium lauryl sulfate on rust removal at 25 °C are shown in Table S4. Supplementary information is available at www.ias.ac.in.

Acknowledgements

This work was supported by Jilin Province Science and Technology Development Plan project (20180201019SF), and the Doctor Startup Foundation of Jilin Institute of Chemical Technology.

References

1. Evans U R 1972 Mechanism of rusting under different conditions *Br. Corros. J*. **7** 10
2. Negm N A, Ghuiba F M and Tawfik S M 2011 Novel isoxazolium cationic Schiff base compounds as corrosion inhibitors for carbon steel in hydrochloric acid *Corros. Sci*. **53** 3566
3. Zhang S, Tao Z, Li W and Hou B 2009 The effect of some triazole derivatives as inhibitors for the corrosion of mild steel in 1 M hydrochloric acid *Appl. Surf. Sci*. **255** 6757
4. Collazo A, Nóvoa X R and Pérez C 2010 The corrosion protection mechanism of rust converters: An electrochemical impedance spectroscopy study *Electrochim. Acta* **55** 6156
5. Barchiche C, Sabot R, Jeannin M and Refait Ph 2010 Corrosion of carbon steel in sodium methanoate solutions *Electrochim. Acta* **55** 1940
6. Likens G E, Driscoll C T and Buso D C 1996 Long-term effects of acid rain: response and recovery of a forest ecosystem *Science* **272** 224
7. Bentiss F, Traisnel M and Lagrenee M 2000 Inhibitor effects of triazole derivatives on corrosion of mild steel in acidic media *Br. Corros. J*. **35** 315
8. Ai J Z, Guo X P and Qu J E 2006 Adsorption behavior and synergistic mechanism of a cationic inhibitor and KI on the galvanic electrode *Colloids. Surf. A* **281** 147
9. Ajmal M, Rawat J and Quraishi M A 1999 Thioamidines as novel class of corrosion inhibitors *Br. Corros. J*. **34** 220
10. Negm N A and Zaki M F 2008 Corrosion inhibition efficiency of nonionic Schiff base amphiphiles of *p*-aminobenzoic acid for aluminum in 4 N HCl *Colloids. Surf. A* **322** 97
11. Solmaz R, Kardas G, Yazlcl B and Erbil M 2008 Adsorption and corrosion inhibitive properties of 2-amino-5-mercapto-1,3,4-thiadiazole on mild steel in hydrochloric acid media *Colloids. Surf. A* **312** 7
12. Avci G 2008 Corrosion inhibition of indole-3-acetic acid on mild steel in 0.5 M HCl *Colloids. Surf. A* **317** 730
13. Keera S T and Deyab M A 2005 Effect of some organic surfactants on the electrochemical behavior of carbon steel in formation water *Colloids. Surf. A*. **266** 129
14. Moura E F, Neto A O W, Dantas T N C, Júnior S H and Gurgel A 2009 Applications of micelle and microemulsion systems containing aminated surfactants synthesized from ricinoleic acid as carbon-steel corrosion inhibitors *Colloids. Surf. A* **340** 199
15. Hossain S A and Almarshad A I 2006 Inhibiting effect of thiosemicarbazide on cold rolled carbon steel *Corros. Eng. Sci. Tech*. **41** 77
16. Zeng F L, Tan X, Li J F and Zhang Z 2013 Corrosion inhibition of A3 steel by imidazoline derivative in 2.0% NaCl solution *Corros. Eng. Sci. Tech*. **48** 108
17. Fuchs-Godec R 2006 The adsorption, CMC determination and corrosion inhibition of some N-alkyl quaternary ammonium salts on carbon steel surface in 2 M H_2SO_4 *Colloids. Surf. A* **280** 130
18. Fuchs-Godec R and Dolecek V 2004 A effect of sodium dodecylsulfate on the corrosion of copper in sulphuric acid media *Colloids. Surf. A* **244** 73
19. Li X G, Huang M R and Zeng J F 2004 The preparation of polyaniline waterborne latex nanoparticles and their films with anti-corrosivity and semi-conductivity *Colloids. Surf. A* **248** 111
20. Mikhailova S S and Povstugar V I 2004 Surfactant protective layers on the surface of nanocrystalline iron particles *Colloids. Surf. A* **239** 77

21. Yang M, Wang Z M, Han X and Zhang J 2017 Corrosion inhibition by the trace amount of sulphide ion in CO_2-saturated brine solutions *Corros. Eng. Sci. Tech*. **52** 73
22. Wojnicki M and Kwolek P 2019 Spectrophotometric study of corrosion inhibition of aluminium in orthophosphoric acid aqueous solutions by using sodium molybdate *Corros. Eng. Sci. Tech*. **54** 199
23. Sastri V S, Packwood R H, Brown J R, Bednar J S, Galbraith L E and Moore V E 1989 Corrosion inhibition by some oxyanions in coal-water slurries *Br. Corros. J*. **24** 30
24. Asefi D, Arami M, Sarabi A A and Mahmoodi N M 2009 The chain length influence of cationic surfactant and role of nonionic co-surfactants on controlling the corrosion rate of steel in acidic media *Corros. Sci*. **51** 1817
25. Yang J Y, Wang D D and Qiao R J 2019 Evaluation of corrosion inhibition performance of two novel multi-functional silane containing phosphonyl groups synthesized by convenient Mannich reaction *Chem. Select.* **4** 972
26. Tan B, Zhang S, Li W, Zuo X, Qiang Y, Xu L, Hao J and Chen S 2019 Experimental and theoretical studies on inhibition performance of Cu corrosion in 0.5 M H_2SO_4 by three disulfide derivatives *J. Ind. Eng. Chem*. **75** 449
27. Li X H, Deng S D and Fu H 2009 Adsorption and inhibition effect of 6-benzylaminopurine on cold rolled steel in 1.0 M HCl *Electrochim. Acta* **54** 4089
28. Noor E A 2005 The inhibition of mild steel corrosion in phosphoric acid solutions by some N-heterocyclic compounds in the salt form *Corros. Sci.* **47** 33
29. Zheng X, Zhang S, Gong M and Li W 2014 Experimental and theoretical study on the corrosion inhibition of mild steel by 1-Octyl-3-methylimidazolium $_L$-Prolinate in sulfuric acid solution *Ind. Eng. Chem. Res.* **53** 16349
30. Nathiya R S and Raj V 2017 Evaluation of Dryopteris cochleata leaf extracts as green inhibitor for corrosion of aluminium in 1 M H_2SO_4 *Egypt. J. Petrol*. **26** 313
31. Mehdipour M, Ramezanzadeh B and Arman S Y 2015 Electrochemical noise investigation of Aloe plant extract as green inhibitor on the corrosion of stainless steel in 1 M H_2SO_4 *J. Ind. Eng. Chem*. **21** 318
32. Li X, Deng S, Xie X and Fu H 2014 Inhibition effect of bamboo leaves' extract on steel and zinc in citric acid solution *Corros. Sci*. **87** 15
33. Odewunmi N A, Umoren S A and Gasem Z M 2015 Utilization of watermelon rind extract as a green corrosion inhibitor for mild steel in acidic media *J. Ind. Eng. Chem.* **21** 239
34. Singh A, Lin Y, Ebenso E E, Liu W, Pan J and Huang B 2015 Gingko biloba fruit extract as an eco-friendly corrosion inhibitor for J55 steel in CO_2 saturated 3.5% NaCl solution *J. Ind. Eng. Chem*. **24** 219
35. Suedile F, Robert F, Roos C and Lebrini M 2014 Corrosion inhibition of zinc by Mansoa alliacea plant extract in sodium chloride media: Extraction, Characterization and Electrochemical Studies *Electrochim. Acta* **133** 631
36. Kolb H C, Finn M G and Sharpless K B 2001 Click chemistry: diverse chemical function from a few good reactions *Angew. Chem. Int. Ed*. **40** 2004
37. Goldmann A S, Walther A, Nebhani L, Joso R, Ernst D, Loos K, Barner-Kowollik C, Barner L and Muller A H E 2009 Surface modification of poly (divinylbenzene) microspheres via thiol-ene chemistry and alkyne-azide click reactions *Macromolecules* **42** 3707
38. Zhang M M and Liang G L 2018 Applications of CBT-Cys click reaction: past, present, and future *Sci. China Chem*. **61** 1088
39. Garg S M, Xiong X B, Lu C and Lavasanifar A 2011 Application of click chemistry in the preparation of poly (ethylene oxide)-block-poly (ε- caprolactone) with hydrolyzable cross-links in the micellar core *Macromolecules* **44** 2058
40. Luo K, Yang J Y, Kopeckova P and Kopecek J 2011 Biodegradable multiblock poly [*N*-(2-hydroxypropyl) methacrylamide] via reversible addition-fragmentation chain transfer polymerization and click chemistry *Macromolecules* **44** 2481
41. Lowe A B 2010 Thiol-ene "click" reactions and recent applications in polymer and materials synthesis *Polym. Chem*. **1** 17